Asymmetric Modular Synthesis of a Semirigid Dipeptide Mimetic by Cascade Cycloaddition/Ring Rearrangement and Borohydride Reduction

Sara Pellegrino,*[†] Alessandro Contini,[†] Maria Luisa Gelmi,[†] Leonardo Lo Presti,[‡,§] Raffaella Soave,[‡,§] and Emanuela Erba[†]

[†]Università degli Studi di Milano, DISFARM-Sez. Chimica Generale e Organica "A.Marchesini", via Venzian 21, 20133 Milano, Italy
[‡]Università degli Studi di Milano, Dipartimento di Chimica, Via Golgi 19, 20133 Milano, Italy
[§]CNR- Istituto di Scienze e Tecnologie Molecolari, Via Golgi 19, 20133 Milano, Italy

Ⓢ *Supporting Information*

ABSTRACT: A new semirigid dipeptide mimetic was prepared on multigram scale, in good yield, and in a stereocontrolled way, starting from commercially available and unexpensive reagents, i.e., *N*-benzylpiperidone, tosyl azide, and proline methyl ester. The optimized multicomponent process consisted of a cascade click cycloaddition and a ring rearrangement reaction, followed by a reductive step. Theoretical calculations were performed to elucidate the reaction mechanism and support the stereochemical outcome of the reduction. Finally, the new scaffold was used for the preparation of model peptidomimetics, whose β turn conformation was confirmed by dynamic NMR experiments.
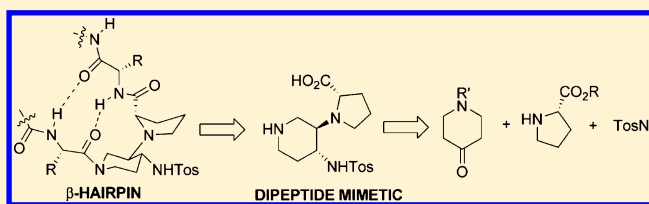
INTRODUCTION

Peptidomimetics are small synthetic molecules able to mimic peptides and protein fragments. Intense research has been made on their development in the early 21st century.[1] The design and preparation of peptidomimetics able to selectively perturb protein−protein interactions (PPI) is, in particular, an important challenge for both chemical biology and medicinal chemistry.[2] The most applied approach is the use of rigid scaffolds mimicking the secondary structure of the binding portion involved in PPI.[3] On the other hand, extreme rigidity is desirable only if the obtained molecular shape is exactly complementary to the binding partner, but most often PPIs rely on an induced fit of the two interacting units. In order to fit in the target, it is now commonly assessed that peptidomimetics should have several kinetically and thermodynamically accessible local minima representing conformations. As a result, the use of semirigid mimetics of secondary protein structures is a much more convenient approach.[4]

The most prevalent nonrepetitive motif observed in proteins is the four residues β turn, in which Pro and Gly are generally found in the *i*+1 and *i*+2 positions.[5] Many rigid scaffolds mimicking this structural motif have been developed,[6] and the Pro-D-Pro or D-Pro-Pro sequences have demonstrated the effective semirigid reverse turn nucleators.[7] More recently, the D-Pro-Pro motif has also been inserted into several peptides to be used as low-loading organocatalysts, providing higher catalytic activity and stereoselectivity than proline itself.[8]

In this work, a semirigid dipeptide mimetic **1**, containing piperidine and a NH-tosyl-functionalized pyrrolidine, was designed and synthesized. An efficient protocol, consisting of

a cascade click cycloaddition and ring rearrangement reactions, followed by a reductive step, was developed. Our challenge was the preparation of **1** on a gram scale, controlling the stereochemistry of the new stereocenters and without the isolation of any intermediates (Scheme 1). Theoretical

Scheme 1. Retrosynthesis of Reverse-Turn Peptidomimetic
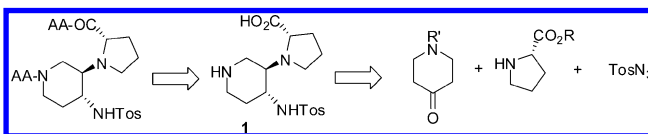
calculations were performed to elucidate the reaction mechanism and supported the stereochemical outcome. Finally, compound **1** was used for the preparation of model peptidomimetics, whose conformation was studied by NMR technique.

RESULTS AND DISCUSSION

Synthesis of Dipeptide Mimetics. Our researches have been focused on the reactions between sulfonylazides and enamines for a long time.[9] We recently reported on a multicomponent click reaction between morpholine, 1-methyl-4-piperidone, and tosyl azide affording azacycloalkene *N*-monosulfonyl diamines, formed through a 5-amino-1,2,3-triazoline rearrangement.[9a] As proline is involved in β turn

**Scheme 2. Mechanism of Multicomponent Reaction**
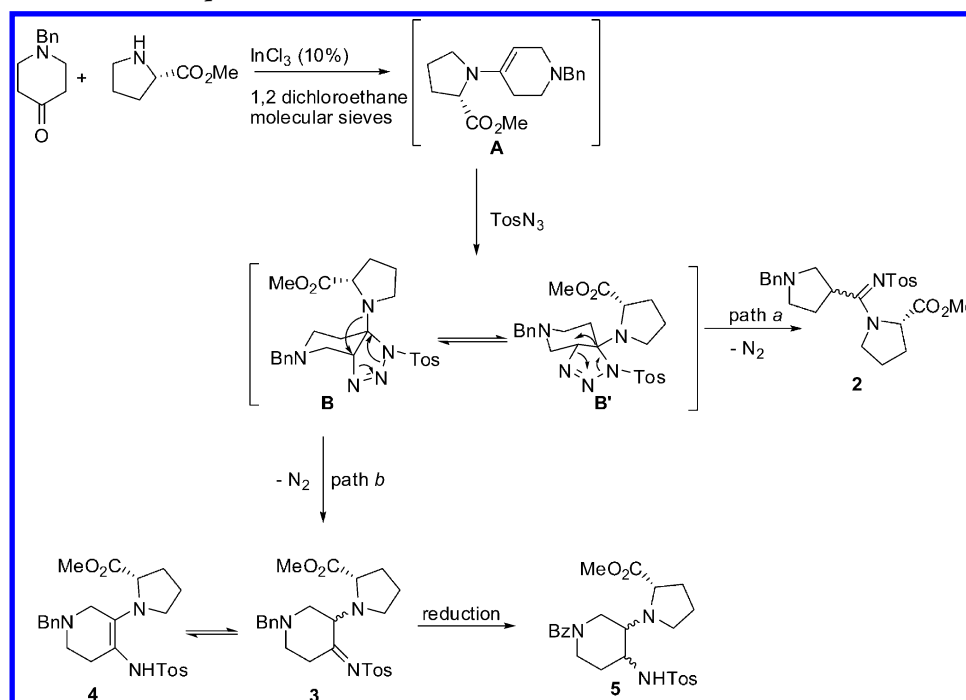
induction, we envisioned the possibility to use this amino acid as a secondary amine instead of morpholine, in order to obtain enantiopure compound **1** (Scheme 1).

The robustness of the above reaction was checked using commercially available *N*-benzylpiperidone, tosyl azide, and proline methyl ester hydrochloride. First, the hydrochloride salt was neutralized using TEA (1 equiv) in 1,2 dichloroethane. *N*-Benzylpiperidone, molecular sieves, and after 1 h, tosyl azide (1 equiv) were added to the mixture, but the reaction did not occur. In order to overcome eventual issues in the formation of the enamine, a catalytic amount of InCl$_3$ was added to the initial mixture of the ketone and the free amine. The sulfonyl azide was then dropped, and the reaction was complete after 45 min (TLC analysis). Any attempt to purify the crude reaction mixture by crystallization failed, while it was possible to isolate only a mixture of diasteroisomeric amidines **2** (20%) by column chromatography (Scheme 2).

The compound **2** isolation was proof that the cycloaddition/ ring rearrangement reactions were effective. As in the recently reported mechanism for morpholino derivatives,[9a] proline reacts first with keto compound (leading to enamine **A**) and then reacts with tosyl azide, affording cycloadduct **B** in equilibrium with its conformer **B′**. Amidines **2** are formed through a concerted transposition of the piperidine ring bond and nitrogen elimination (path a). As the main products were degraded during the workup, our hypothesis is that, starting from conformer **B**, the concerted transposition of proline moiety and nitrogen elimination (path b) gives imine **3**. The latter equilibrates to azacycloalkene diamine derivative **4**, which was not stable during the purification on silica gel (Scheme 2).

Since compounds **5** were our synthetic targets, we reasoned that the direct treatment of the multicomponent reaction mixture with a reducing agent could give access to a more stable piperidine ring. (Scheme 2) In compounds **3/4**, the reduction of the double bond of could give four isomers: two having a *trans* substitution pattern and the others with *cis* disposition, respectively (Figure 1). Our interest was the control of the

reduction stereochemical outcome; thus, we tested different reducing agents.
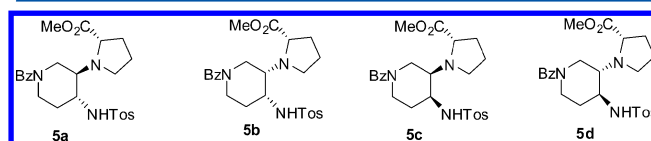
Figure 1. Possible stereoisomers of **5**.

We first performed a catalytic hydrogenation using Pd/C in MeOH (1 atm, 25 °C), which actually led to a complex mixture (^{1}H NMR). Molecular weights, corresponding to amidines **2** and piperidines **5**, together with their *N*-debenzylated derivatives, were detected in the mass spectrum of the crude. In order to avoid the formation of mixtures and the *N*-benzyl deprotection side reaction, we then turned to borohydride reducing agents.[10] As reported,[10b] by tuning the sterical and electronic properties of the substituents on the boron atom, it could be possible to control the diastereoselection in the formation of the new stereocenters.

A series of reducing borohydrides were tested. The reactions were directly performed on the crude click reaction mixture, operating at 25 °C for 10 h. Using NaBH(OAc)$_3$ (2.5 equiv), the reaction was successful (40% overall yield), leading exclusively to **5a** and **5b** isomers, together with amidine **2** (**5a/5b/2**, 2:1:1 ratio, ^{1}H NMR and HPLC analyses, see the Supporting Information). The same stereochemical outcome was found with NaBH$_3$CN (2.5 equiv), obtaining the only **5a** and **5b** isomers, although their distribution was found not completely reproducible. Only degradation products were observed using NaBH$_4$ (2.5 equiv). The reaction did not occur with 2.5 equiv of hindered L-Selectride. A complex reaction mixture was obtained by increasing the equivalents (5 equiv) of the reducing agent (**2/5a/5b/5c,d** 3:2:1:1, LC/MS analysis of the crude).

Scheme 3. Scale up of Multicomponent Reaction
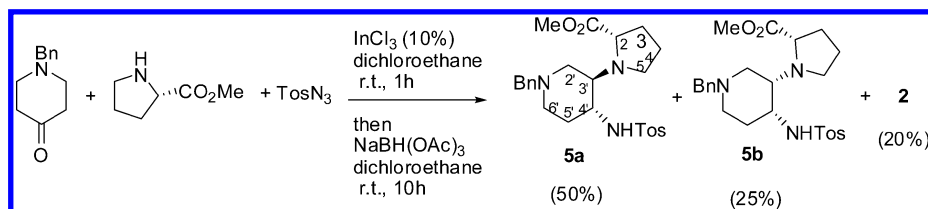
NaBH(OAc)$_3$ was thus selected as the best catalyst to control the diastereoselection. In order to enhance the yield, we increased the amount of the reducing agent (5 eq instead of 2.5 equiv), obtaining compounds **5** in 75% yield (**5a**/**5b**, 2:1).

Finally, the entire protocol was carried out on a multigram scale (4 g of proline). The multicomponent reaction between the proline, N-benzylpiperidone, and tosyl azide was first performed. After removal of the solvent and molecular sieves, dichloroethane and NaBH(OAc)$_3$ (5 equiv) were added, and the mixture was allowed to sit for 10 h at 25 °C under stirring. After column chromatography, compound **5a** was isolated in good yield (50%) with the minor isomer **5b** (25%) and amidine **2** (20%) (Scheme 3).

The stereochemistry of compounds **5a** and **5b** was assigned by NMR analyses. The NOESY spectrum of **5a** showed a spatial proximity between H3′ and NHTos protons, suggesting a *trans* configuration of the Pro and NHTos substituents on the piperidine ring. On the other hand, this spatial proximity was not found for isomer **5b**. X-ray analysis on **5a** confirmed the *trans* configuration of the substituents, indicating a *R* configuration of both C3′ and C4′ stereocenters and the *S* configuration of Cα of Pro (see the Supporting Information, Figure S1). On the contrary, crystal structure of stereoisomer **5b** showed the *S* and the *R* configuration of the C3′ and the C4′, respectively (see the Supporting Information, Figure S6). Thus, stereoisomers **5a** and **5b** possess the same stereochemistry at C4′.

To explain the stereochemical outcome on the reduction, insights on the reaction mechanism were acquired.

First, it can be safely assumed that between tautomers **3** and **4** the former is the most reactive toward hydrides, as the negative charge deriving from the nucleophilic attack at **3**-C4′ can be delocalized on the more electronegative sulfonamide group, while on **4** it would be delocalized on carbon (Scheme 4). Second, it can be hypothesized that the hydride only attacks at the *Re* face, thus leading to the *R* configuration of C4′. The variability at C3′ should instead depend on the thermodynamic

Scheme 4. Hypothesized Mechanism for Hydride Attack on Tautomers 3 and 4
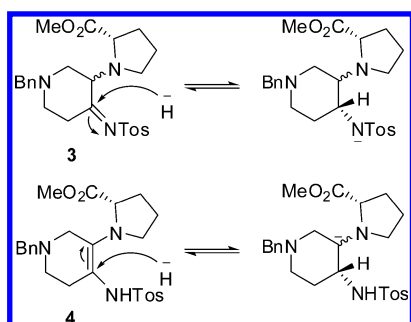
stability of the 3′*R* and 3′*S* diastereoisomeric imides **3**, which are in equilibrium due to tautomerization between **3** and **4**.

Our interest focuses on theoretical analyses of chemical reactions,[9a,11] and DFT calculations were thus done to explain the reasons for the observed stereochemistry. Indeed, a study on the mechanism and diastereoselectivity of NaBH$_4$ reduction of ketones was published by Suzuki and co-workers.[12] They reported that DFT calculations were able to describe the geometry and energy of the stationary point along the reaction path and correctly predict the diastereoisomeric ratio of the reduction of 4-methylcyclohexanone, which showed a preference for the *trans* isomer, and 2-*tert*-butylcyclohexanone, where diastereoselectivity was almost eliminated. In these cases, diastereoselection was observed to be dependent from the difference in energy between the two transition states (TS) obtained from the axial or equatorial attack of the hydride on cyclohexanone. Interestingly, the authors reported that the inclusion of the Na$^+$ counterion in the theoretical models was essential to reproduce the experimental results. Indeed, they demonstrated that NaBH$_4$ is associated and Na$^+$ ion takes an active part in the TS even by using methanol as the solvent. Starting from these findings, we thought of applying to our system the model by Suzuki et al. Some approximations needed to be done for reasons of feasibility. In particular, to reduce both the size and degrees of freedom of the system, the benzyl at N1 and the tolyl at SO$_2$ were replaced by methyl groups. The effect of this simplification was evaluated by performing a conformational search, at the molecular mechanics (MM) level, on the approximated model of **5a** (M5a) and by comparing the results with the X-ray structure of **5a**. A root-mean-square deviation (RMSD) of 0.52 Å was obtained between the heavy atoms of M5a most stable conformation and the corresponding atoms of **5a**, suggesting that such approximation is not critical (Figure S9, Supporting Information). TS models for both the axial and equatorial hydride attack on models (3′*R*)-**3** and (3′*S*)-**3**, leading to all possible diastereoisomers, were located by considering NaBH$_3$CN as the reducing agent. By using NaBH(OAc)$_3$, convergence time was unacceptably long. Since the two reactants substantially led to comparable stereochemical results, our simplification can be considered acceptable. Single-point energy calculations were performed on optimized geometries at the mPW1B95/6-311G(2d,p) level both in the gas phase and in dichloroethane.

The obtained relative energies are summarized in Table 1 (see the Supporting Information for absolute energies), while selected geometrical parameters are reported in Table 2. Geometries of all TSs deriving from either the axial or the equatorial attack of the hydride are depicted in Figure 2.

First of all, the most stable structures, TS-3′*R*,4′*R*-ax and TS-3′*S*,4′*R*-ax, led to the actually isolated compounds **5a** and **5b**, although gas-phase calculations predict both TSs to be energetically equivalent. Conversely, single-point energy calculations conducted in solution by using the PCM model

Table 1. Relative Gibbs Free Energies (kcal/mol) Computed at the mPW1B95/6-311G(2d,p) Level for TSs Leading to (3′R,4′R), (3′S,4′R′), (3′R,4′S), and (3′S,4′S) Configurations of M5[a]

model	$\Delta\Delta G^{\ddagger}_{gas}$	$\Delta\Delta G^{\ddagger}_{DCE}$
TS-3′R,4′R-ax	0.0	0.0
TS-3′R,4′R-eq	10.1	2.3
TS-3′S,4′R-ax	0.0	0.5
TS-3′S,4′R-eq	6.2	5.0
TS-3′R,4′S-ax	1.6	2.2
TS-3′R,4′S-eq	3.0	1.4
TS-3′S,4′S-ax	9.2	4.9
TS-3′S,4′S-eq	9.3	3.3

[a]Gibbs free energies are computed by single-point calculations at the mPW1B95/6-311G(2d,p) level on geometries optimized at the mPW1B95/6-31G(d) level in the gas phase and include thermochemical corrections from vibrational analysis conducted at the same level of theory in standard conditions (1 atm, 298.15 K). Relative activation free energies are obtained as the difference between the energy computed for the considered TS and that of the most stable one.

provide excellent concordance with the experiments, with a $\Delta\Delta G^{\ddagger}$ = 0.5 kcal/mol in favor of the most abundant regioisomer **5a** (**5a:5b** = 2:1).

The second observation deriving from theoretical results is that the axial attack of the hydride is the most favored for all the examples in the gas phase, while the axial attack is still favored in solution for those paths leading to the experimentally obtained compounds **5a** and **5b**. Considering that, for the herein reported examples, NaBH(OAc)$_3$ and NaBH$_3$CN provided comparable results in terms of product stereo- and regiochemistry, a similar mechanism of attack could be hypothesized. Our findings are thus apparently in contrast with the general observation that bulky reducing agents usually favor equatorial attack.[10b] However, our results are probably due to the peculiar substitution pattern of the substrate. Concerning TS-3′R,4′R, in the most favored axial TS, the bulky substituents at C3′ and C4′ are both in an equatorial position (Figure 3), and no evident steric interference is found by analyzing the TS geometry (see Figure S10, Supporting Information). Moreover, the TS is stabilized by electrostatic

interactions between the Na$^+$ ion and (i) the partially negative charged sulfonamide nitrogen (see Scheme 4), (ii) the proline nitrogen, (iii) the carbonyl group, (iv) the SO$_2$ oxygen, and (v) the electron-rich CN group of the borohydride (see Table 2).

Conversely, in the equatorial TS, the two substituents at C3′ and C4′ are both axial, and only three stabilizing interactions are found between the Na$^+$ ion and electron-rich groups (see Figure 3 and Table 2). Moreover, the equatorial approach of the reducing agent to the substrate is hampered by steric hindrances of the methoxycarbonyl group of proline, the SO$_2$ group, and the axial hydrogen at C5′ (see Figure S10, Supporting Information).

For TS-3′S,4′R, no particular differences are observed among axial and equatorial TSs on the steric hindrance, hampering the approach of the reducing agent to the substrate. However, in the equatorial TS geometry the S(O$_2$)N···C≡N distance is 2.81 Å, while 3.31 Å is measured in the axial TS. This would suggest that there is on the former TS, a stronger repulsive effect between the electron-rich sulphonamide nitrogen and the CN group. Moreover, steric interferences are also observed between the proline hydrogen atoms at Cα and Cδ and those at C2′, C3′, and C4′ of the piperidine ring, less relevant in the corresponding axial TS (Figure S11, Supporting Information).

Concerning TS-3′R,4′S, which does not lead to experimentally isolated products, the two approaches, axial and equatorial, are closer in terms of relative activation energies. The former is favored by 1.4 kcal/mol in the gas phase and the second is favored by 0.8 kcal/mol in solution and only 1.4 kcal/mol less stable than TS-3′R,4′R. Although the difference is small, it is enough to make it impossible to obtain experimentally the product, according to the Arrhenius equation.[13] Both axial and equatorial TSs pay an energy toll probably due to unfavorable steric contacts that are between the methoxycarbonyl and sulfonamide methyl groups and between the boron-linked hydrogen and the proline Hα (see Figure 3).

Even for the least stable TS-3′S,4′S, the axial TS is predicted as slightly favored in the gas phase, while in solution the equatorial attack is preferred, although it is still 3.3 kcal/mol less stable than the most favored TS-3′R,4′R axial. Probably, the higher energy is mainly due to the stabilizing interaction

Table 2. Selected Geometrical Parameters of Optimized TSs

|	TS-3′R,4′R		TS-3′S,4′R		TS-3′R, 4′S		TS-3′S,4′S	
	axial	equat	axial	equat	axial	equat	axial	equat
distances (Å)								
C4′−H	1.12	1.12	1.13	1.12	1.12	1.12	1.12	1.12
H4′−B	2.03	2.09	2.09	1.97	2.09	2.06	2.07	2.09
B−NSO$_2$	2.78	3.56	3.70	2.78	3.72	3.77	2.80	3.66
S(O$_2$)N−Na	2.38	2.33	2.39	2.31	2.46	2.31	2.36	2.34
OSO−Na	2.32	2.23	2.25	2.30	2.25	2.40	2.25	2.23
C≡N−Na	2.50	2.39	2.48	2.53	2.43	2.78	2.50	2.38
N(Pro)−Na	2.93	5.92	4.24	2.73	4.21	2.66	2.51	5.89
C=O−Na	2.24	6.70	2.24	2.27	2.23	2.33	5.32	7.01
angles (deg)								
C4′−H4′−B	126.0	141.8	161.8	129.0	163.3	163.9	125.7	152.6
C=O−Na	116.2	79.8	129.3	120.0	115.3	108.8	47.0	95.6
C≡N−Na	96.7	112.9	119.0	95.4	119.4	106.7	95.6	116.4
C3′−N(Pro)−Na	106.4	32.3	63.2	106.0	67.2	109.8	112.2	35.4
C4′−N−Na	124.0	131.6	130.9	125.4	130.4	116.3	113.6	128.5
S=O−Na	94.1	95.8	97.0	96.2	97.4	92.2	94.9	95.4
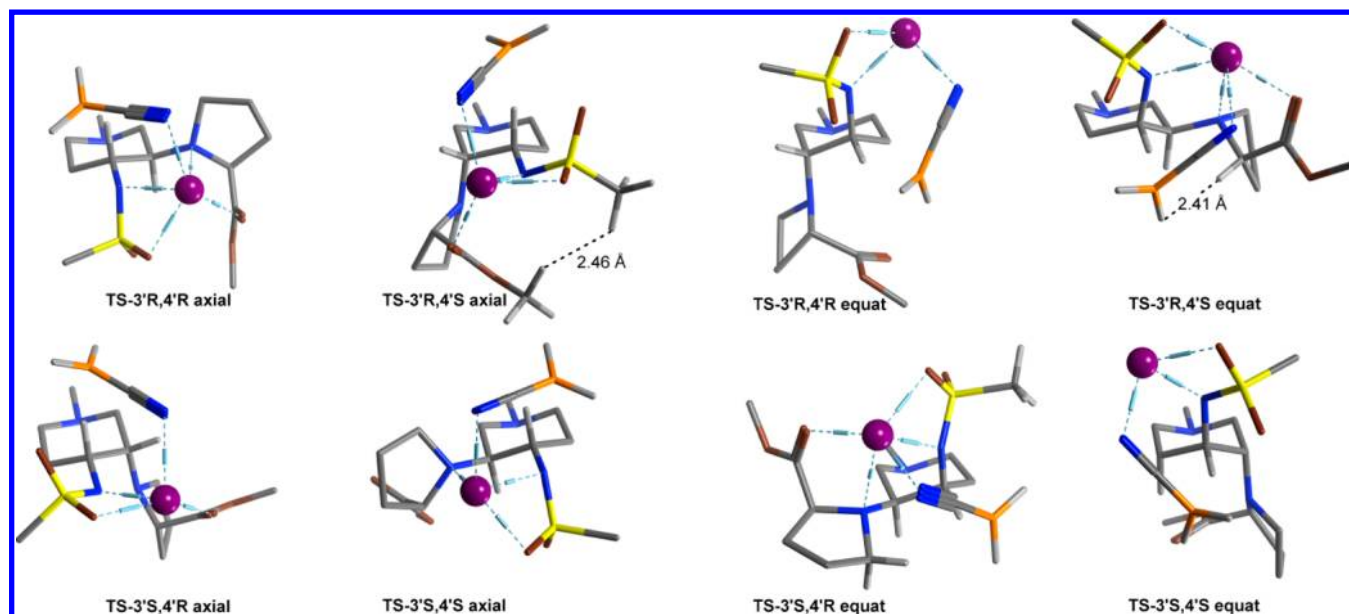
Figure 2. Geometries of all of the possible TSs deriving from either the axial or equatorial attack of the hydride.
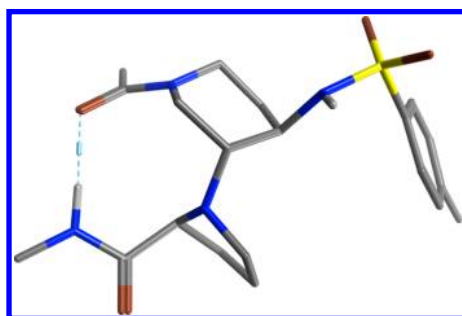

Figure 3. β-Turn-like geometry of dipeptide model **7** obtained by conformational search.

between the methoxycarbonyl group and the Na⁺ ion, which is missing in both the axial and equatorial TSs: a singularity among the cases analyzed herein.

Taken together, the theoretical data suggest that the stereo- and regiochemical outcome observed experimentally can be ascribed to a fine balance of steric and electronic factors. The latter is dependent from the interactions between the electron-rich functional groups and the Na⁺ ion, whose role is again predicted to be extremely relevant as suggested by Suzuki et al.[12]

Peptidomimetic Synthesis. From the crystal structure of both compounds **5a** and **5b** (Figure S1 and S6, Supporting Information), it was evidenced that the carboxylic group of Pro and the benzyl substituent on the piperidine ring were oriented in the same direction. The spatial proximity between Cα of Pro and the benzyl group suggested that both scaffolds could act as a β turn nucleator when inserted into a peptide sequence. A preliminary conformational search conducted on the dipeptide model **7**, deriving from the major isomer **5a**, encouraged us to pursue this idea, since a top-ranked conformation presented a β turn-like geometry with an H-bond between the proline amide NH and the acetamide carbonyl group at N1′ forming a 10-membered ring (Figure 3). Furthermore, the computed phy and psi values of Pro, were in the range of a type VIII β turn.

In order to confirm this hypothesis, the preparation of dipeptide **7** was planned both to ascertain by NMR the correct

orientation of the chains and to develop the most efficient protocol for peptidomimetic synthesis. Starting from **5a**, the "one pot" catalytic hydrogenation/acetylation reaction was performed using toluene as the solvent and adding Ac₂O (2 equiv) to the reaction mixture. Compound **6** was obtained in moderate yield (40%) and then treated with MeNH₂ in EtOH at 0 °C affording **7** (50%, Scheme 5).

Scheme 5. Synthesis of Dipeptide Model 7
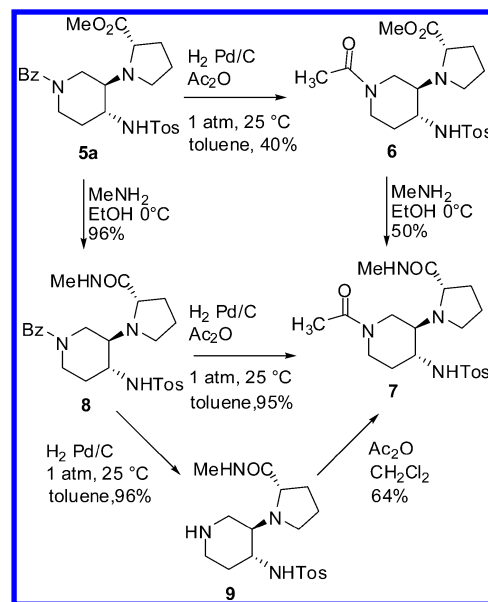
To improve the yield, we tested a second synthetic protocol, consisting first of the functionalization of the carboxylic group and then of the deprotection of nitrogen. Compound **5a** was thus treated with MeNH₂ in EtOH at 0 °C obtaining compound **8** (96%) and then deprotected with H₂, Pd/C in toluene. The obtained free amine **9** (96%) was acetylated using Ac₂O, affording compound **7** (64%). When the reduction was carried out in the presence of Ac₂O, the yield was increased (95% instead of 60% in two steps) (Scheme 5).

Scheme 6. Synthesis of Peptidomimetic 13
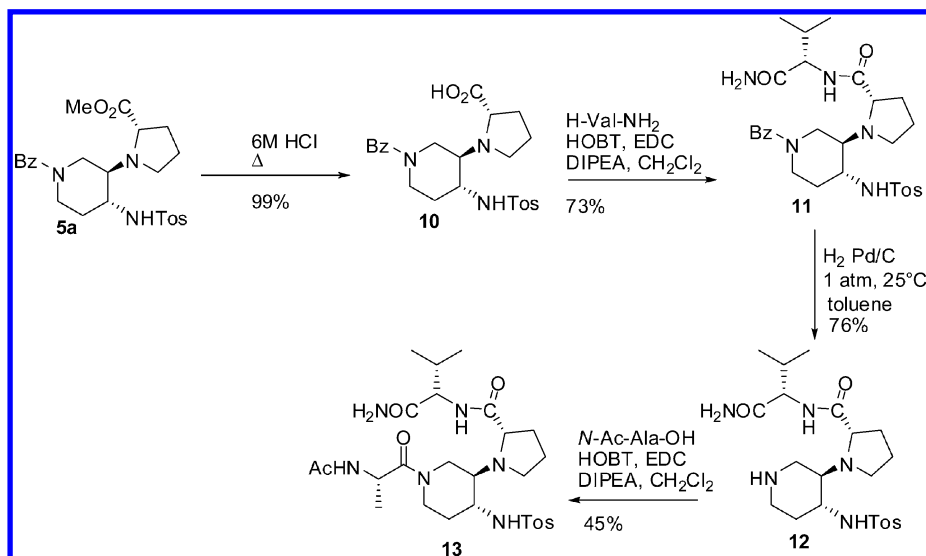
We tested the possibility of using compound **5a** in the synthesis of short peptide models. According to the above best synthetic protocol, peptidomimetic **12** was synthesized by hydrolysis of compound **5a** (6 M HCl), affording free carboxylic acid **10** (99%). Its coupling with H-Val-NH$_2$ using HOBT, EDC as coupling reagents, DIPEA as the base, and CH$_2$Cl$_2$ as the solvent (10 h) (Scheme 6) gave compound **11** (72%). The latter was then debenzylated to derivative **12** (76%). Peptidomimetic **13** (45%) was finally obtained by coupling of **12** with N-Ac-Ala-OH using the above conditions (Scheme 6).

NMR Discussion. Compound **7** was characterized by means of 1D and 2D NMR experiments (20 mM in CD$_3$CN, 25 °C, 500 MHz), as well as by dynamic NMR experiments (0–60 °C temperature range in CD$_3$CN). The 1D ^{1}H spectrum showed the presence of two different conformers **7** and **7′** (1:1 ratio, Figure 5 and Table S1 and S2, Supporting Information). Performing the ^{1}H NMR analysis in DMSO, the complete coalescence of the signals was observed at 80 °C. Dynamic NMR experiments in CD$_3$CN showed in both isomers a high temperature coefficient for NHTos, while NHMe was involved in a medium-weak hydrogen bond only in **7** (see Tables S2 and S3, Supporting Information). In the NOESY experiments, both conformers showed spatial proximities between the Hα of Pro and H6′, while an NOE effect between Hα of Pro and H2′ was observed only for the hydrogen bonded isomer **7**. On the other hand, the isomer **7′** showed a spatial proximity between Hα of Pro and NHMe (Figure 4) From these findings, we can postulate that the two conformers **7** and **7′** could correspond to the rotamers of the acetamide bond, as typically found in similar compounds.[14] We suggested that a reverse turn
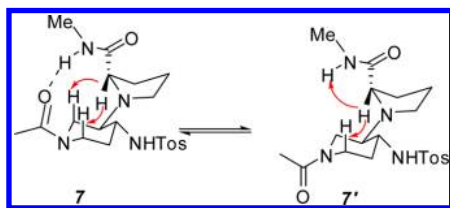
conformation is active for isomer **7**, which is stabilized by the hydrogen bond. The latter consideration is also supported by the observation that compound **6**, which possesses an acetyl group on piperidine ring and an ester function on Pro, exists as a single conformer in solution and shows no significant Overhauser effect in the NOESY experiments, thus lacking a reverse-turn conformation.

Peptidomimetic **13** is present in solution as a mixture of two conformers **13/13′** (1:1 ratio, Figure 5, Tables S3 and S4,
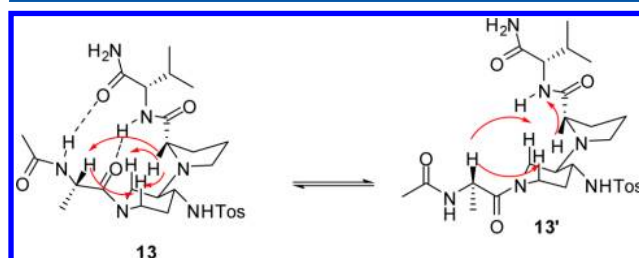

Figure 5. Schematic representation of conformers **13** and **13′** supported by NOE experiments.

Supporting Information). In isomer **13**, NH-Val and the NH-acetyl are involved in medium-weak hydrogen bonds (see Tables S3 and S4, Supporting Information), while none of the amidic protons of **13′** showed low temperature coefficients. In the NOESY experiments, both conformers **13** and **13′** showed spatial proximity between the Hα of Ala and H2′ and H6′. On the contrary, Overhauser effects between Hα of Pro and H2′ and H6′ were present only for the hydrogen bonded conformer **13**, while spatial proximity between Hα of Pro and NH-Val was found in isomer **13′**. These findings suggested that a β turn conformation is present in conformer **13**, while **13′** possesses an extended conformation.

In conclusion, starting from commercially available cheap reagents, through a multicomponent/cascade process, the new scaffold **5a** was prepared in multigram scale, in good yield, and with a good control in the formation of two new stereocenters. When inserted into a peptide chain, compound **5a** acts as a β turn nucleator, representing a promising building block that contains an additional amino group on the piperidine ring, which could be used for further functionalization of the ring.

Figure 4. Schematic representation of conformers **7** and **7′** supported by NOE experiments.

Furthermore, the semirigid structure of compound **5a** is an added value for its use in the preparation of PPI modulators.

■ EXPERIMENTAL SECTION

Materials and solvents were purchased from common commercial sources and used without additional purification. ^1H NMR spectra were recorded at 200, 400, or 500 MHz and ^{13}C NMR spectra at 50, 70, or 125 MHz using TMS as internal standard. The following abbreviations were used to describe peak patterns where appropriate: singlet (s), doublet (d), triplet (t), multiplet (m), broad resonances (br). Coupling constants (J) are reported in hertz. Mass spectra were recorded under electron spray interface (ESI) conditions. Infrared spectra were recorded on a FTIR spectrometer. $[\alpha]_D$ values were measured using CHCl$_3$ as the solvent, if not differently reported.

Theoretical Calculations. Transition states were fully optimized at the mPW1B95/6-31G(d) level of theory.[15] Different conformations were evaluated for each structure, and only the most stable was further considered. Vibrational frequencies were computed at the same level of theory in order to verify the presence of unique imaginary frequency corresponding to the vibrational stretching of the forming/breaking bonds and to calculate zero-point and thermochemical corrections to electronic energies (1 atm, 298.15 K, unscaled frequencies). Single-point calculations were then performed at the 6-311G(2d,p) level, both in the gas phase and in solution, by using the PCM solvent model for dichloroethane.[16] All quantum chemical calculations were performed with the Gaussian09 software package.[17] Conformational searches were conducted in the gas phase by using the MOE software with the MMFF94x force field and default parameters.

Multicomponent Reaction Procedure. To a suspension of proline methyl ester hydrochloride (4 g, 24 mmol) in 1,2 dichloroethane (40 mL) was added TEA (3.36 mL, 1 equiv). After 15 min, under N$_2$ atmosphere, 4-benzylpiperidone (4.2 mL, 24.0 mmol) and molecular sieves (5 g) were added to the solution. After 30 min, a catalytic amount of InCl$_3$ (0.53 g, 0.1 equiv) was added, and stirring was continued for 45 min. The reaction mixture was cooled at 10 °C, and tosyl azide (4.76 g, 24.0 mmol) dissolved in dichloroethane (20 mL) was added. After 45 min (TLC analysis: CH$_2$Cl$_2$/CH$_3$OH, 20:1), (AcO)$_3$BHNa (25.4 g, 5 equiv) was added to the crude that was allowed to stir for 12 h at 25 °C (TLC analysis: CH$_2$Cl$_2$/AcOEt, 1:1). The reaction mixture was filtered, washed with water (3 × 30 mL), and dried with Na$_2$SO$_4$, and the solvent was removed under vacuum. The crude was crystallized with CH$_3$OH obtaining pure **5a** (2.2 g, 20%). The mother liquor was purified by column chromatography (CH$_2$Cl$_2$/AcOEt from 100:0 to 50:50) affording a further amount of **5a** (3.2 g, 30%), together with amidine **2** (2.15 g, 20%) and **5b** (2.19 g, 20%).

S-Methyl 1-[(1-Benzylpyrrolidin-3-yl-(tosylimido)methyl)]-pyrrolidine-2-carboxylate (2). Mixture of inseparable diastereoisomers: IR (KBr) 3247, 2917, 2250, 1740 cm^{-1}; ^1H NMR (CDCl$_3$, 200 MHz) δ 1.60–1.98 (m, 2H), 1.99–2.35 (m, 3H), 2.36–2.54 (m, 2H), 2.40 (s, 3H), 2.55–2.75 (m, 1H), 3.00–3.20 (m, 2H), 3.45 (s, 3H), 3.55–3.95 (m, 3H), 4.05–4.35 (m, 1H), 4.36–4.55 (m, 2H), 7.20–7.41 (m, 7H), 7.72 (d, *J* 7.4 Hz, 2H); ^{13}C NMR (CDCl$_3$, 50 MHz) δ 21.6, 25.7 (25.4), 28.6, 29.9, 40.6, 48.9, 52.0, 54.5, 55.2, 59.9, 62.3, 126.4, 127.5 (127.7), 128.6, 128.9, 129.1 (130.1), 138.6 (C), 141.9 (141.6) (C), 167.8 (C), 172.1 (C); MS (ESI) M$^+$ 470. Anal. Calcd for C$_{25}$H$_{31}$N$_3$O$_4$S: C, 63.94; H, 6.65; N, 8.95. Found: C, 63.72; H, 6.77; N, 8.72.

S-Methyl 1-[(3R,4R)-1-Benzyl-4-tosylamido-piperidin-3-yl]-pyrrolidine-2-carboxylate (5a). White solid; mp 156–157 °C (MeOH); $[\alpha]_D$ = 108.3 (*c* 0.4, 20 °C); IR (KBr) 3202, 2937, 1739 cm^{-1}; ^1H NMR (CDCl$_3$, 500 MHz) δ 1.34–1.45 (m, 1H),1.49–1.72 (m, 2H), 1.73–2.10 (m, 5H), 2.22–2.38 (m, 2H), 2.42 (s, 3H), 2.57–2.64 (m, 1H), 2.68–2.84 (m, 3H), 3.40–3.59 (m, 3H), 3.79 (s, 3H), 6.82 (bs, 1H), 7.15–7.31 (m, 7H), 7.80 (d, *J* 8.2 Hz, 2H); ^{13}C NMR (CDCl$_3$, 125 MHz) δ 20.8, 23.7 (CH$_2$), 29.1, 32.1, 43.5, 50.9, 51.1, 51.7, 52.9, 57.8, 61.3, 62.3, 126.5, 126.6, 127.6, 128.2, 128.6, 136.8, 137.1, 142.1, 175.4; MS (ESI) M$^+$ 472. Anal. Calcd for C$_{25}$H$_{33}$N$_3$O$_4$S: C, 63.67; H, 7.05; N, 8.91. Found: C, 63.49; H, 7.46; N, 8.67.

S-Methyl 1-[(3S,4R)-1-Benzyl-4-tosylamidopiperidin-3-yl]-pyrrolidine-2-carboxylate (5b). Yellow solid: mp 95–97 °C (*i*-Pr$_2$O); $[\alpha]_D$ = (*c*, 20 °C); IR (KBr) 3256, 2921, 1736 cm^{-1}; NMR (CDCl$_3$, 500 MHz) δ 1.37–1.42 (m, 1H), 1.67–1.72 (m, 1H), 1.79–2.10 (m, 6H), 2.43 (s, 3H), 2.59–2.63 (m, 1H), 2.70–2.75 (m, 1H), 2.85–2.94 (m, 3H), 2.96–3.00 (m, 1H), 3.48 (s, 2H), 3.60 (s, 3H), 3.63 (dd, *J* 7.7, 3.7 Hz, 1H), 5.85 (bs, 1H), 7.20–7.35 (m, 7H), 7.78 (d, *J* 7.2 Hz, 2H). ^{13}C NMR (CDCl$_3$, 125 MHz) δ 21.5, 23.8, 29.6, 30.5, 49.3, 51.4, 51.5, 52.0, 54.1, 60.0, 60.3, 62.8, 127.2, 127.3, 128.3, 129.0, 129.4, 137.7, 138.4, 143.1, 175.6; MS (ESI) M$^+$ 472. Anal. Calcd for C$_{25}$H$_{33}$N$_3$O$_4$S: C, 63.67; H, 7.05; N, 8.91. Found: C, 63.40; H, 7.30; N, 8.61.

S-Methyl 1-[(3R,4R)-1-Acetyl-4-tosylamidopiperidin-3-yl]-pyrrolidine-2-carboxylate (6). To a solution of **5a** (0.2 g, 0.4 mmol) and acetic anhydride (0.052 g, 0.44 mmol) in toluene (20 mL) was added Pd/C (10%, 0.1 g), and the obtained suspension was stirred under H$_2$ at room temperature for 12h. The mixture was filtered through a Celite pad, and the solvent was removed under vacuum affording pure compound **6** (0.07 g, 40%) as a colorless gum: IR (KBr) 320, 1740 cm^{-1}; ^1H NMR (CDCl$_3$, 300 MHz) δ 1.30–1.62 (m, 3H, 1.66–1.85 (m, 2H), 1.99–2.11 (m, 1H), 2.05 (s, 3H), 2.32–2.60 (m, 4H), 2.44 (s, 3H), 2.82–3.10 (m, 2H), 3.77 (s, 3H), 3.40–3.78 (m, 2H), 4.55 (d, *J* 9.6 Hz, 1H), 7.00 (bs, 1H, exch), 7.30 (d, *J* 9.9 Hz, 2H), 7.79 (d, *J* 6.4 Hz, 2H); ^{13}C NMR (CDCl$_3$, 50 MHz) δ 21.7, 21.9, 24.9, 30.7, 34.2, 40.5, 44.3, 45.2, 52.8, 54.1, 58.4, 62.4, 127.6, 129.4, 137.6, 137.7, 143.4, 169.5, 176.6; MS (ESI) M$^+$ 423. Anal. Calcd for C$_{20}$H$_{29}$N$_3$O$_5$S: C, 56.72; H, 6.90; N, 9.92. Found: C, 56.55; H, 7.10; N, 9.73.

S-N-Methyl 1-[(3R,4R)-1-Acetyl-4-tosylamido)piperidin-3-yl]-pyrrolidine-2-carboxamide (7). Method A: Operating at 0 °C and under N$_2$ atmosphere, pure isomer **6** (0.34g, 0.85 mmol) was dissolved in CHCl$_3$ (2 mL), and then methylamine (8 M in EtOH, 15 mL) was added. After 1 h, the mixture was warmed at room temperature and the stirring was continued overnight. The solvent was evaporated, and pure compound **7** was obtained after crystallization from hexane (0.17 g, 50%). Method B: To a solution of **8** (0.36 g, 0.75 mmol) in toluene (20 mL) were added acetic anhydride (0.153 g, 1.5 mmol) and Pd/C (10%, 0.08g). The suspension was stirred under H$_2$ atmosphere at room temperature for 12 h. The reaction mixture was filtered through a Celite pad, and the solvent was removed under vacuum. Pure compound **7** (0.33 g, 95%) was obtained as a white powder after crystallization from hexane. Method C: Pure compound **9** (58 mg, 0.15 mmol) was dissolved in CH$_2$Cl$_2$ (10 mL) and Ac$_2$O (51 mg, 1 mmol) was added. The solution was left under stirring at room temperature for 5 h. The solvent was removed affording and pure **7** was obtained after crystallization from hexane (40 mg, 64%): IR (KBr) 3425, 3271, 1659 cm^{-1}; $[\alpha]_D$ = −62.1 (*c* 0.3, 20 °C); mp 60–62 °C (hexane); ^1H NMR (CD$_3$CN, 300 MHz) 1:1 mixture of conformers, δ 1.21–1.80 (m, 4H), 1.99–2.55 (m, 6H), 2.00 (s, 3H), 2.44 (s, 3H), 2.73, 2.75 (2 s, 3H), 2.81–3.30 (m, 2H), 3.33–3.46 (m, 1H), 3.65–3.87 (m, 1H), 4.43–4.53 (m, 1H), 6.99, 7.11 (2 bs, 1H, exch), 7.15 (bs, 1H, exch.), 7.39 (d, *J* 8.0 Hz, 2H), 7.79 (d, *J* 8.2 Hz, 2H); ^{13}C NMR (CD$_3$CN, 75 MHz) 1:1 mixture of conformers δ 20.9, 24.5 (24.6), 25.6, 30.8 (30.9), 33.9, 40.0, 44.3 (44.4), 44.9, 53.9 (54.0), 58.8, 59.6, 64.0, 127.0, 129.9, 138.5, 143.7, 168.9, 175.9; MS (ESI) M$^+$ 423. Anal. Calcd for C$_{20}$H$_{30}$N$_4$O$_4$S: C, 56.85; H, 7.16; N, 13.26. Found: C, 56.68; H, 7.30; N, 13.01.

S-N-Methyl1-[(3R,4R)-1-Benzyl-4-tosylamidopiperidin-3-yl]-pyrrolidine-2-carboxamide (8). Pure isomer **5a** (0.4 g, 0.85 mmol) was dissolved in CHCl$_3$ (2 mL). Methylamine (8 M in EtOH, 15 mL) was added at 0 °C and under N$_2$ atmosphere. After 1 h, the ice bath was removed and the stirring continued overnight. The solvent was evaporated to yield pure compound **8** (0.38g, 98%) as a yellow powder after crystallization from Et$_2$O: IR (KBr) 3307, 3087, 1655 cm^{-1}; $[\alpha]_D$ = −75.0 (*c* 0.4, 20 °C); mp 80–82 °C (Et$_2$O); ^1H NMR (CDCl$_3$, 200 MHz) δ 1.37–2.25 (m, 7H), 2.40 (s, 3H), 2.42–2.95 (m, 5H), 2.8 (d, *J* 5.14 Hz, 3H), 3.00–3.22 (m, 1H), 3.41 (d, *J* 11.0 Hz, 1H), 3.47 (d, *J* 11.0 Hz, 1H), 5.28 (bs, 1H), 7.18–7.38 (m, 7H), 7.62 (bs, 1H, exch), 7.77 (d, *J* 8.1 Hz, 2H); ^{13}C NMR (CDCl$_3$, 50 MHz) δ 21.7, 25.1, 26.1, 31.4, 32.5, 45.4, 51.9, 52.1, 54.2, 60.5, 62.9, 64.4, 127.1, 127.5, 128.5,

129.1, 129.8, 137.7, 138.7, 143.4, 176.2 MS (ESI) M⁺ 471. Anal. Calcd for $C_{25}H_{32}N_4O_4S$: C, 61.96; H, 6.66; N, 11.56. Found: C, 61.81; H, 6.89; N, 11.32.

S-N-Methyl-1-[(3R,4R)-4-Tosylamido)piperidin-3-yl]pyrrolidine-2-carboxamide (9). To a solution of **8** (0.29 g, 0.63 mmol) in toluene (20 mL) was added Pd/C (10%, 0.13 g), and the suspension was stirred for 12h under H₂ at room temperature. The crude was filtered through a Celite pad, and the solvent was removed under vacuum obtaining pure compound **9** (0.2g, 96%) after crystallization from toluene: IR (KBr) 3436, 3271, 3176, 1658 cm⁻¹; $[\alpha]_D = -55.6$ (*c* 0.6, 20 °C); mp 195−197 °C (toluene); ¹H NMR (CDCl₃, 300 MHz) δ 1.25−1.45 (m, 1H), 1.55−1.73 (m, 2H), 1.75−1.91 (m, 2H), 1.95−2.13 (m, 1H), 2.22 (bs, 2H), 2.31−2.50 (m, 2H), 2.44 (s, 3H), 2.51−2.71 (m, 2H), 2.74−2.86 (m, 1H), 2.73 (d, *J* 4.9 Hz, 3H), 2.86−2.97 (m, 1H), 3.0−3.12 (m, 1H), 3.20 (dt,, *J* 9.1, 4.7 Hz, 1H), 3.40 (dd, *J* 9.6, 4.0 Hz, 1H), 7.32 (d, *J* 8.1 Hz, 2H), 7.64 (bs, 1H, exch), 7.80 (d, *J* 8.3 Hz, 2H); ¹³C NMR (CDCl₃, 75 MHz) δ 21.9, 25.2, 26.3, 31.6, 34.9, 44.8, 45.5, 45.7, 54.7, 61.8, 64.8, 127.3, 130.1, 138.8, 143.8, 176.2; MS (ESI) M⁺ 381. Anal. Calcd for $C_{18}H_{28}N_4O_3S$: C, 56.82; H, 7.42; N, 14.72. Found: C, 56.59; H, 7.70; N, 14.48.

S 1-[(3R,4R)-1-Benzyl-4-tosylamidopiperidin-3-yl]pyrrolidine-2-carboxylic Acid HCl (10). In a sealed tube, pure isomer **5a** (0.1 g, 0.21 mmol) was dissolved in 6 N HCl (2 mL) and heated at 110 °C in oil bath. The solution was stirred for 4 h and then evaporated yielding pure compound **10** (0.95g, 99%) as a white solid: FTIR (KBr) 3435, 3270, 1631 cm⁻¹; $[\alpha]_D = -35$ (*c* 0.6 in MeOH, 20 °C); mp 95−97 °C (Et₂O); ¹H NMR (D₂O, 200 MHz) δ 1.42−1.63 (m, 2H), 1.79−2.19 (m, 3H), 2.30 (s, 3H), 2.22−2.33 (m, 1H), 2.78−3.00 (m, 1H), 3.19−3.45 (m, 2H), 3.50−3.82 (m, 3H), 4.19−4.25 (m, 1H), 4.26, (d, *J* 13.2 Hz, 1H), 4.33 (d, *J* 13.2 Hz, 1H), 7.25−7.50 (m, 7H), 7.70 (d, *J* 8.5 Hz, 2H); ¹³C NMR (D₂O, 50 MHz) δ 21.0, 24.0, 27.1, 28.8, 48.3, 49.7, 50.3, 50.4, 60.0, 61.4, 67.3, 127.1, 129.8, 130.8, 131.0, 131.6, 127.8, 135.4, 146.4, 172.1; MS (ESI) M⁺ 458. Anal. Calcd for $C_{24}H_{29}N_3O_5S$: C, 61.13; H, 6.20; N, 8.91. Found: C, 60.81; H, 6.53; N, 8.65.

(S)-N-((S)-1-Amino-3-methyl-1-oxobutan-2-yl)-1-((3R,4R)-1-benzyl-4-tosylamidopiperidin-3-yl)pyrrolidine-2-carboxamide (11). To a solution of **10** (99 mg, 0.22 mmol) in CH₂Cl₂ (15 mL) and DMF (2 mL) were added HOBT (35 mg, 0.26 mmol) and EDC (49 mg, 0.26 mmol). The solution was stirred for 1 h at 0 °C. (*S*)-Valinamide (36 mg, 0.24 mmol) and DIPEA (0.15 g, 87 mmol) were added. The mixture was stirred overnight at room temperature and washed with water (10 mL) and with a saturated solution of NaHCO₃ (10 mL). The organic layer was dried with Na₂SO₄ and evaporated under vacuum to yield **11** (0.89g, 73%) as a yellow powder: FTIR (KBr) 3435, 2962, 1661 cm⁻¹; $[\alpha]_D = -53$ (*c* 0.3, 20 °C); mp 70−73 °C (Et₂O); ¹H NMR (CD₃CN, 300 MHz) δ 0.94 (d, *J* 6.7 Hz, 3H), 0.97 (d, *J* 6.7 Hz, 3H), 1.40−1.85 (m, 5H), 1.86−2.25 (m, 3H), 2.42 (s, 3H), 2.40−2.60 (m, 2H), 2.68−2.75 (m, 1H), 2.85−3.10 (m, 1H), 3.20−3.35 (m, 2H), 3.38−3.75 (m, 2H), 4.22−4.29 (m, 1H), 6.17 (bs, 1H), 6.68 (bs, 1H), 7.25−7−55 (m, 8H), 7.77 (d, *J* 8.2 Hz, 2H), 7.88 (bs, 1H); ¹³C NMR (CD₃CN, 75 MHz) δ 18.0, 19.4, 20.9, 24.7, 30.7, 31.3, 33.5, 44.8, 51.0, 51.9, 54.2, 57.6, 58.7, 62.2, 63.6, 127.0, 127.7, 128.7, 129.S, 130.0, 138.2, 140.1, 143.6, 174.9, 175.5; MS (ESI) M⁺ 556. Anal. Calcd for $C_{29}H_{41}N_5O_4S$: C, 62.68; H, 7.44; N, 12.60. Found: C, 62.92; H, 7.21; N, 12.43.

(S)-N-((S)-1-Amino-3-methyl-1-oxobutan-2-yl)-((3R,4R)-4-tosylamidopiperidin-3-yl)pyrrolidine-2-carboxamide (12). To a solution of **11** (50 mg, 0.09 mmol) in toluene (5 mL) Pd/C (10%, 0.05 g) was added. The suspension was stirred under H₂ atmosphere at room temperature for 30 h. The catalyst was filtered through a Celite pad that was carefully washed with methanol (20 mL). The solvent was evaporated under vacuum yielding pure compound **12** (0.032g, 76%) as a light yellow powder after crystallization from hexane: IR (KBr) 3435, 2963, 1662 cm⁻¹; $[\alpha]_D = -24.3$ (*c* 0.2, 20 °C); mp 57−59 (hexane); ¹H NMR (CD₃CN, 200 MHz) δ 0.94 (d, *J* 6.7 Hz, 3H), 0.97 (d, *J* 6.7 Hz, 3H), 1.19−1.35 (m, 1H), 1.40−1.85 (m, 6H), 1.86−2.19 (m, 3H), 2.25−2.60 (m, 4H), 2.42 (s, 3H), 2.65−2.85 (m, 1H), 2.90−3.10 (m, 1H), 3.33 (dd, *J* 9.9, 4.8 Hz, 1H), 4.27 (dd, *J* 9.9, 6.7 Hz, 1H), 6.17 (bs, 1H), 6.68 (bs, 1H), 7.25−7.55 (m, 3H), 7.77 (d, *J* 8.4 Hz, 2H), 7.90 (d, *J* 10.2 Hz, 1H); ¹³C NMR (CD₃CN, 50 MHz) δ

17.8, 19.2, 20.7, 23.5, 24.6, 30.6, 31.2, 43.7, 44.6, 45.3, 54.7, 57.3, 60.0, 63.5, 126.8, 128.5, 140.2, 143.4, 175.0, 175.4; MS (ESI) M⁺ 466. Anal. Calcd for $C_{22}H_{35}N_5O_4S$: C, 56.75; H, 7.58; N, 15.04. Found: C, 56.50; H, 7.90; N, 14.85.

(S)-1-((3R,4R)-1-((S)-2-Acetamidopropanoyl)-4-(tosylamidopiperidino-3-yl)-N-((S)-1-amino-3-methyl-1-oxobutan-2-yl)pyrrolidine-2-carboxamide (13). To a cooled solution of N-acetyl-(*S*)-alanine (16 mg, 0.121 mmol) in CH₂Cl₂ (5 mL) were added HOBT (16 mg, 0.121 mmol) and EDC (23 mg, 0.121 mmol). The mixture was stirred for 1 h, and **12** (47 mg, 0.101 mmol) was added. The solution was stirred overnight at room temperature, washed with water (10 mL) and a saturated solution of NaHCO₃ (10 mL), and then dried over Na₂SO₄. The solvent was evaporated under vacuum affording **13** (26 mg, 45%) as a white powder: $[\alpha]_D = +34.5$ (*c* 0.5, 20 °C); mp 62−64 °C (Et₂O); ¹H NMR 1:1 mixture of conformers (CD₃CN, 300 MHz) δ 0.83 (d, *J* 6.7 Hz, 3H), 0.97 (d, *J* 6.7 Hz, 3H),1.15−1.19 (m, 3 H),1.49−1.55 (m, 1H), 1.66−1.70 (m, 2H), 1.91 (s, 3H) 2.04−2.13 (m, 2H), 2.19−2.35 (m, 3H), 2.38 (s, 3H), 2.41−2.54 (m, 3H), 2.91−3.01 and 2.97−3.12 (two m, 1H), 3.18−3.23 and 3.23−3.38 (two m, 1H), 3.43−3.68 (m, 1H), 3.74−3.85 and 3.86−3.98 (two m, 1H), 4.24−4.36 (m, 1H), 4.31−4.38 and 4.45−4.56 (two m, 1H), 4.66−4.76 (m, 1H), 6.11 (bs, 1H, exch), 6.60 (bs, 1H, exch), 6.75 (d, *J* 7.2 Hz, 1H, exch), 7.28 (bs, 1H, exch), 7.38 (d, *J* 8.0 Hz, 2H), 7.76 and 7.87 (two bs, 1H, exch), 7.78 (d, *J* 6.6 Hz, 2H); ¹³C NMR (CD₃CN, 75 MHz) δ 17.9, 18.3, 19.3, 20.9, 22.3, 24.7 (24.8), 30.7 (30.9), 31.5 (31.4), 34.5 (33.5), 39.7 (41.1), 43.4 (44.1), 44.7 (44.6), 45.1 (45.2), 54.4 (54.2), 57.6 (57.4), 58.7 (59.2), 63.5 (63.4), 127.1, 130.0, 139.8, 143.7, 169.5 (169.2), 171.0, 174.8, 175.2; MS (ESI) M⁺ 577.5. Anal. Calcd for $C_{27}H_{42}N_6O_6S$: C, 56.04; H, 7.31; N, 14.52. Found: C, 55.81; H, 7.60; N, 14.32.

■ ASSOCIATED CONTENT

Ⓢ Supporting Information

X-ray data for **5a** and **5b** (CIF); tables with significant NMR data for compounds 7, 7′, 13, and 13′; HPLC spectra of multicomponent reaction and of compounds 2, 5a, and 5b; ¹H, ¹³C NMR spectra for all new compounds; NOESY spectra of compounds 7 and 13; computational details; crystallographic description; tables of the atomic coordinates of compounds **5a** and **5b**. This material is available free of charge via the Internet at http://pubs.acs.org.

■ AUTHOR INFORMATION

Corresponding Author

*E-mail: sara.pellegrino@unimi.it.

Notes

The authors declare no competing financial interest.

■ ACKNOWLEDGMENTS

■ REFERENCES

(1) (a) Kostova, M. B.; Rosen, D. M.; Chen, Y.; Mease, R. C.; Denmeade, S. R. *J. Med. Chem.* **2013**, *56*, 4224−4235. (b) Suwal, S.; Kodadek, T. *Org. Biomol. Chem.* **2013**, *11*, 2088−2092. (c) Pellegrino, S.; Ruscica, M.; Magni, P.; Vistoli, G.; Gelmi, M. L. *Bioorg. Med. Chem.* **2013**, *21*, 5470−5479. (d) Hanessian, S.; Chénard, E. *Org. Lett.* **2012**, *14*, 3222−3225. (e) Singh, S.; Sieburth, S. M. *Org. Lett.* **2012**, *14*, 4422−4425. (f) Pellegrino, S.; Contini, A.; Clerici, F.; Gori, A.; Nava, D.; Gelmi, M. L. *Chem.—Eur. J.* **2012**, *18*, 8705−8715. (g) Pedersen, D. S.; Abell, A. *Eur. J. Org. Chem.* **2011**, *2011*, 2399−2411. (h) Ung, P.; Winkler, D. A. *J. Med. Chem.* **2011**, *54*, 1111−1125. (i) Yoo, B.; Shin, S. B. Y.; Huang, M. L.; Kirshenbaum, K. *Chem.—Eur. J.* **2010**, *16*, 5528−5537. (j) Pellegrino, S.; Ferri, N.; Colombo, N.; Cremona, E.;

Corsini, A.; Fanelli, R.; Gelmi, M. L.; Cabrele, C. *Bioorg. Med. Chem. Lett.* **2009**, *19*, 6298−6302.

(2) (a) Harvey, S. R.; Porrini, M.; Stachl, C.; MacMillan, D.; Zinzalla, G.; Barran, P. E. *J. Am. Chem. Soc.* **2012**, *134*, 19384−19392. (b) Whitby, L. R.; Boger, D. L. *Acc. Chem. Res.* **2012**, *45*, 1698−1709. (c) Vidal, M.; Cusick, M. E.; Barabási, A.-L. *Cell* **2011**, *144*, 986−998. (d) Buchwald, P. *IUBMB Life* **2010**, *62*, 724−731.

(3) (a) Grauer, A.; König, B. *Eur. J. Org. Chem.* **2009**, *2009*, 5099−5111. (b) Vagner, J.; Qu, H.; Hruby, V. J. *Curr. Opin. Chem. Biol.* **2008**, *12*, 292−296.

(4) Ko, E.; Raghuraman, A.; Perez, L. M.; Ioerger, T. R.; Burgess, K. *J. Am. Chem. Soc.* **2012**, *135*, 167−173.

(5) Hutchinson, E. G.; Thornton, J. M. *Protein Sci.* **1994**, *3*, 2207−2216.

(6) (a) Nair, R. V.; Kotmale, A. S.; Dhokale, S. A.; Gawade, R. L.; Puranik, V. G.; Rajamohanan, P. R.; Sanjayan, G. J. *Org. Biomol. Chem.* **2014**, *12*, 774−782. (b) Thorat, V. H.; Ingole, T. S.; Vijayadas, K. N.; Nair, R. V.; Kale, S. S.; Ramesh, V. V. E.; Davis, H. C.; Prabhakaran, P.; Gonnade, R. G.; Gawade, R. L.; Puranik, V. G.; Rajamohanan, P. R.; Sanjayan, G. J. *Eur. J. Org. Chem.* **2013**, *2013*, 3529−3542. (c) Lesma, G.; Cecchi, R.; Cagnotto, A.; Gobbi, M.; Meneghetti, F.; Musolino, M.; Sacchetti, A.; Silvani, A. *J. Org. Chem.* **2013**, *78*, 2600−2610. (d) Ottersbach, P. A.; Schmitz, J.; Schnakenburg, G.; Gütschow, M. *Org. Lett.* **2013**, *15*, 448−451. (e) Wu, C.-F.; Zhao, X.; Lan, W.-X.; Cao, C.; Liu, J.-T.; Jiang, X.-K.; Li, Z.-T. *J. Org. Chem.* **2012**, *77*, 4261−4270. (f) Reuter, C.; Huy, P.; Neudörfl, J.-M.; Kühne, R.; Schmalz, H.-G. *Chem. —Eur. J.* **2011**, *17*, 12037−12044. (g) Ko, E.; Burgess, K. *Org. Lett.* **2011**, *13*, 980−983. (h) Eckhardt, B.; Grosse, W.; Essen, L.-O.; Geyer, A. *Proc. Natl. Acad. Sci. U.S.A.* **2010**, *107*, 18336−18341. (i) Fuller, A. A.; Du, D.; Liu, F.; Davoren, J. E.; Bhabha, G.; Kroon, G.; Case, D. A.; Dyson, H. J.; Powers, E. T.; Wipf, P.; Gruebele, M.; Kelly, J. W. *Proc. Natl. Acad. Sci. U.S.A.* **2009**, *106*, 11067−11072.

(7) Feng, J.; Tessler, L.; Marshall, G. *Int. J. Pept. Res. Ther.* **2007**, *13*, 151−160.

(8) (a) Kastl, R.; Wennemers, H. *Angew. Chem., Int. Ed.* **2013**, *52*, 7228−7232. (b) Duschmalé, J.; Wennemers, H. *Chem. —Eur. J.* **2012**, *18*, 1111−1120.

(9) (a) Contini, A.; Erba, E. *RSC Adv.* **2012**, *2*, 10652−10660. (b) Contini, A.; Erba, E.; Pellegrino, S. *Synlett* **2012**, *23*, 1523−1525. (c) Cassani, F.; Celentano, G.; Erba, E.; Pocar, D. *Synthesis* **2004**, 1041−1046.

(10) (a) Gribble, G. W. *Org. Process Res. Dev.* **2006**, *10*, 1062−1075. (b) Hutchins, R. O.; Su, W. Y.; Sivakumar, R.; Cistone, F.; Stercho, Y. P. *J. Org. Chem.* **1983**, *48*, 3412−3422.

(11) (a) Casoni, A.; Borsini, E.; Contini, A.; Ruffoni, A.; Pellegrino, S.; Clerici, F. *Curr. Org. Chem.* **2011**, *15*, 3514−3522. (b) Gassa, F.; Contini, A.; Fontana, G.; Pellegrino, S.; Gelmi, M. L. *J. Org. Chem.* **2010**, *75*, 7099−7106. (c) Aversa, M. C.; Barattucci, A.; Bonaccorsi, P.; Contini, A. *J. Phys. Org. Chem.* **2009**, *22*, 1048−1057. (d) Borsini, E.; Broggini, G.; Contini, A.; Zecchi, G. *Eur. J. Org. Chem.* **2008**, 2808−2816.

(12) Suzuki, Y.; Kaneno, D.; Tomoda, S. *J. Phys. Chem. A* **2009**, *113*, 2578−2583.

(13) The ratio between to compounds deriving from a kinetically controlled reaction can be obtained as: $[X]/[Y] = ê((\Delta G^{\ddagger}Y − \Delta G^{\ddagger}X)/RT)$; a $\Delta \Delta G^{\ddagger}$ of 1.4 kcal/mol means that the concentration of the most favored product is approximately 10.6 times higher than that of the less favored product.

(14) Laursen, J. S.; Engel-Andreasen, J.; Fristrup, P.; Harris, P.; Olsen, C. A. *J. Am. Chem. Soc.* **2013**, *135*, 2835−2844.

(15) Zhao, Y.; Truhlar, D. G. *J. Phys. Chem. A* **2004**, *108*, 6908−6918.

(16) (a) Klamt, A.; Schüürmann, G. *J. Chem. Soc., Perkin Trans. 2* **1993**, *2*, 799−805. (b) Andzelm, J.; Kölmel, C.; Klamt, A. *J. Chem. Phys.* **1995**, *103*, 9312−9320. (c) Barone, V.; Cossi, M. *J. Phys. Chem. A* **1998**, *102*, 1995−2001. (d) Cossi, M.; Rega, N.; Scalmani, G.; Barone, V. *J. Comput. Chem.* **2003**, *24*, 669−681.

(17) Frisch, M. J.; Trucks, G. W.; Schlegel, H. B.; Scuseria, G. E.; Robb, M. A.; Cheeseman, J. R.; Scalmani, G.; Barone, V.; Mennucci, B.; Petersson, G. A.; Nakatsuji, H.; Caricato, M.; Li, X.; Hratchian, H. P.; Izmaylov, A. F.; Bloino, J.; Zheng, G.; Sonnenberg, J. L.; Hada, M.; Ehara, M.; Toyota, K.; Fukuda, R.; Hasegawa, J.; Ishida, M.; Nakajima, T.; Honda, Y.; Kitao, O.; Nakai, H.; Vreven, T.; Montgomery, J. A., Jr.; Peralta, J. E.; Ogliaro, F.; Bearpark, M.; Heyd, J. J.; Brothers, E.; Kudin, K. N.; Staroverov, V. N.; Kobayashi, R.; Normand, J.; Raghavachari, K.; Rendell, A.; Burant, J. C.; Iyengar, S. S.; Tomasi, J.; Cossi, M.; Rega, N.; Millam, J. M.; Klene, M.; Knox, J. E.; Cross, J. B.; Bakken, V.; Adamo, C.; Jaramillo, J.; Gomperts, R.; Stratmann, R. E.; Yazyev, O.; Austin, A. J.; Cammi, R.; Pomelli, C.; Ochterski, J. W.; Martin, R. L.; Morokuma, K.; Zakrzewski, V. G.; Voth, G. A.; Salvador, P.; Dannenberg, J. J.; Dapprich, S.; Daniels, A. D.; Farkas, Ö.; Foresman, J. B.; Ortiz, J. V.; Cioslowski, J.; Fox, D. J. *Gaussian 09*, Revision D.01 ed.; Gaussian, Inc.: Wallingford, CT, 2013.